can be achieved. (ii) Lesion discrimination seems to result from a kinetic preference to extrude oxoG residues from the DNA helix, relative to normal bases. Should the enzyme occasionally make a mistake and attempt to present a normal base to the active site, that poses no danger, as we have shown, in the case of hOGG1, that the active site has an exquisite ability to discriminate thermodynamically in favor of oxoG (*8*).

References and Notes

1. G. L. Verdine, S. D. Bruner, *Chem. Biol.* **4**, 329 (1997).
2. D. O. Zharkov, A. P. Grollman, *Mutat. Res.* **577**, 24 (2005).
3. L. A. Lipscomb *et al.*, *Proc. Natl. Acad. Sci. U.S.A.* **92**, 719 (1995).
4. Y. Oda *et al.*, *Nucleic Acids Res.* **19**, 1407 (1991).
5. G. E. Plum, A. P. Grollman, F. Johnson, K. J. Breslauer, *Biochemistry* **34**, 16148 (1995).
6. S. S. Parikh, C. D. Putnam, J. A. Tainer, *Mutat. Res.* **460**, 183 (2000).
7. J. T. Stivers, *Prog. Nucleic Acid Res. Mol. Biol.* **77**, 37 (2004).
8. A. Banerjee, W. Yang, M. Karplus, G. L. Verdine, *Nature* **434**, 612 (2005).
9. C. Cao, Y. L. Jiang, J. T. Stivers, F. Song, *Nat. Struct. Mol. Biol.* **11**, 1230 (2004).
10. J. C. Fromme, G. L. Verdine, *J. Biol. Chem.* **278**, 51543 (2003).
11. S. D. Bruner, D. P. Norman, G. L. Verdine, *Nature* **403**, 859 (2000).
12. J. C. Fromme, G. L. Verdine, *Adv. Protein Chem.* **69**, 1 (2004).
13. J. L. Huffman, O. Sundheim, J. A. Tainer, *Mutat. Res.* **577**, 55 (2005).
14. J. Tchou *et al.*, *J. Biol. Chem.* **269**, 15318 (1994).
15. M. Bhagwat, J. A. Gerlt, *Biochemistry* **35**, 659 (1996).
16. S. Boiteux, T. R. O'Connor, F. Lederer, A. Gouyette, J. Laval, *J. Biol. Chem.* **265**, 3916 (1990).
17. D. O. Zharkov, R. A. Rieger, C. R. Iden, A. P. Grollman, *J. Biol. Chem.* **272**, 5335 (1997).
18. F. Coste *et al.*, *J. Biol. Chem.* **279**, 44074 (2004).
19. J. C. Fromme, G. L. Verdine, *Nat. Struct. Biol.* **9**, 544 (2002).
20. R. Gilboa *et al.*, *J. Biol. Chem.* **277**, 19811 (2002).
21. L. Serre, K. Pereira de Jesus, S. Boiteux, C. Zelwer, B. Castaing, *EMBO J.* **21**, 2854 (2002).
22. The oligonucleotides were synthesized using an automated synthesis procedure based on established chemistry (*23*–*25*). The synthesis was carried out on an ABI 392 synthesizer by modifying a regular 1 μM scale synthesis protocol to perform an H-phosphonate coupling step, followed by oxidation using carbon tetrachloride and diamine disulfide (free base) at the site of tether incorporation. (See the supplementary material for additional details.)
23. F. R. Atherton, H. T. Openshaw, A. R. Todd, *J. Chem. Soc.* **1945**, 660 (1945).
24. B. C. Froehler, M. D. Matteucci, *Tetrahedron Lett.* **27**, 469 (1986).
25. R. L. Letsinger, M. E. Schott, *J. Am. Chem. Soc.* **103**, 7394 (1981).
26. A. Banerjee, G. L. Verdine, unpublished data.
27. A. Banerjee, W. L. Santos, G. L. Verdine, data not shown.
28. O. S. Fedorova *et al.*, *Biochemistry* **41**, 1520 (2002).
29. A. A. Ishchenko *et al.*, *Biochemistry* **41**, 7540 (2002).
30. D. T. Gewirth, P. B. Sigler, *Nat. Struct. Biol.* **2**, 386 (1995).
31. C. He *et al.*, *Mol. Cell* **20**, 117 (2005).
32. C. G. Kalodimos *et al.*, *Science* **305**, 386 (2004).
33. H. Viadiu, A. K. Aggarwal, *Mol. Cell* **5**, 889 (2000).
34. F. K. Winkler *et al.*, *EMBO J.* **12**, 1781 (1993).

35. Supported by NIH grant GM044853. For help during data collection and processing, we thank M. Becker and all the staff members at National Synchrotron Light Source beamline X25; C. Heaton, B. Miller, and staff members at Chess A1 beamline; and C. Ogata and N. Sukumar at APS 8BM beamline. We also thank Y. Korkhin for help and advice; Enanta Pharmaceuticals for use of their x-ray facilities for initial characterization of the crystals; and C. Fromme, P. Blainey, and M. Spong for discussions and suggestions on the manuscript. Coordinates and structure factors have been deposited in the Protein Data Bank with accession codes 2F5S (CC1), 2F5Q (CC2), 2F5N (IC1), 2F5P (IC2), and 2F5O (IC3).

Supporting Online Material

www.sciencemag.org/cgi/content/full/311/5764/1153/DC1
Materials and Methods
Figs. S1 to S8
Table S1

19 September 2005; accepted 18 January 2006
10.1126/science.1120288

Coherent Sign Switching in Multiyear Trends of Microbial Plankton

William K. W. Li,* W. Glen Harrison, Erica J. H. Head

Since the 1990s, phytoplankton biomass on the continental shelf of Nova Scotia and in the Labrador Sea has undergone sustained changes in the spring and fall, which are accompanied by changes in bacterioplankton that are dampened in amplitude but coherent in the direction of change. A reversal of trend in biomass change, so-called sign switching, occurs both in time and in space. Thus, whenever (spring or fall) and wherever (Scotian Shelf or Labrador Sea) phytoplankton increase or decrease, so also does bacterioplankton. This tandem sign switch indicates coupling of the trophic levels at a multiyear time scale and contributes to an ecological fingerprint of systemwide forcing.

Sustained monitoring of large ocean ecosystems often reveals systematic changes in phytoplankton abundance. These have been ascribed to systemwide influences such as climate change (*1*) and removal of top predators (*2*). Changes at one trophic level may cascade up or down the food web, and the effects may be discerned when other trophic levels are also monitored (*3*). A large proportion (about 50%) of primary production is routed through the microbial loop in which heterotrophic bacterioplankton assimilate or respire the substrates originating from phytoplankton (*4*). It might thus be inferred that a long-term change in phytoplankton would lead to a concomitant change in bacterioplankton, but we are not aware of any direct evidence at the appropriate time scale.

Here, we show that since the 1990s, phytoplankton biomass on the continental shelf of Nova Scotia and in the Labrador Sea has undergone sustained changes that are accompanied by changes in bacterioplankton, dampened in amplitude but coherent in the direction of change. A reversal of trend in biomass change, so-called sign switching (*5*), occurs both in time (between seasons) and in space (among locations), and the two trophic groups switch sign in tandem. Although heterotrophic and photoautotrophic plankton interact at the short scales of microbial generation times and cellular distances, the ecological relationship between these two trophic groups (at the large scales of a decade and ocean shelves) appears responsive to systemwide forcing.

The Scotian Shelf (SS) has been sampled every spring (April and May) and every fall (October) since 1997 along a western (WSS), a central (CSS), and an eastern (ESS) section, with seven stations on each section comprising the core element of the Canadian Atlantic Zone Monitoring Program (*6*). Additionally, at a single CSS station (HL2, 44.27°N, 63.32°W), there is supplementary sampling once every 2 weeks to delineate higher frequency events. The Labrador Sea has been sampled every spring or early summer (May to July) since 1994 on 28 stations along a section (*7*) starting from Hamilton Bank on the Labrador Shelf (LS), through the central deep Labrador Basin (LB), and ending at Cape Desolation on the Greenland Shelf (GS). At each of the 49 hydrographic stations (fig. S1), we monitor chlorophyll concentration and bacterioplankton abundance (*8*) from the sea surface to 100 m and compute depth-integrated standing stocks of both biotic components. Semimonthly values of surface chlorophyll are also computed throughout the study region with the use of satellite ocean color imagery (*8*).

The biweekly record of depth-integrated chlorophyll concentration at HL2 shows repeated cycles of a major bloom in spring and a minor bloom in fall (Fig. 1A). Over 6 years, average spring chlorophyll (March to May) has been increasing at 14% per year while average fall chlorophyll (September to November) has been decreasing at –9% per year. The same directions of change are also evident in the remotely sensed record of surface chlorophyll (Fig. 1B), abundance of diatoms (Fig. 1C), and abundance of dinoflagellates (Fig. 1D), but with only weak or no statistical significance in all of them (table S1).

Bedford Institute of Oceanography, P.O. Box 1006, Dartmouth, Nova Scotia B2Y 4A2, Canada.

*To whom correspondence should be addressed. E-mail: LiB@mar.dfo-mpo.gc.ca

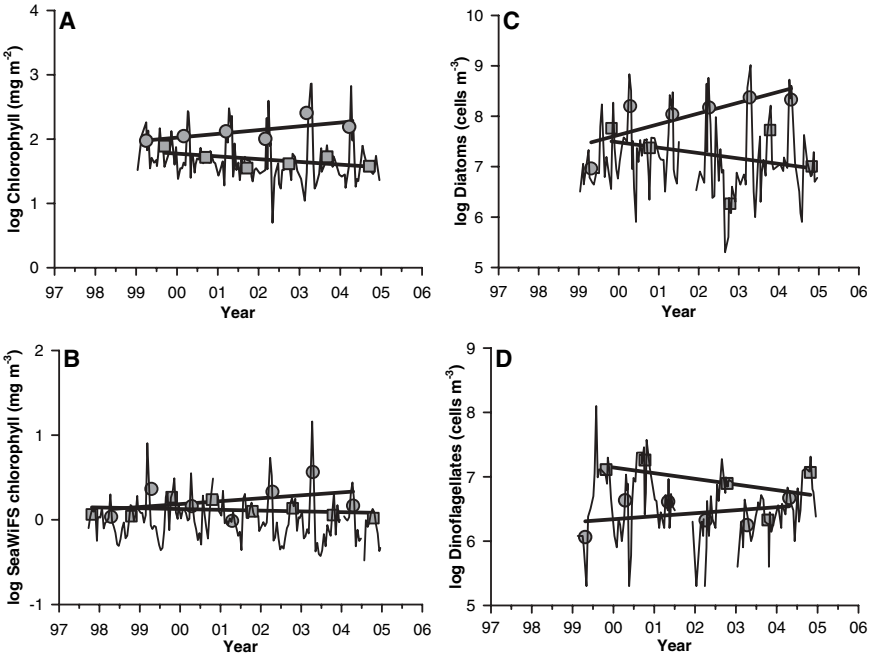

Fig. 1. Time series of phytoplankton at station HL2 in CSS: (**A**) log depth-integrated chlorophyll concentration, (**B**) log SeaWiFS satellite surface chlorophyll concentration, (**C**) log diatom cell concentration, and (**D**) log dinoflagellate cell concentration. Semimonthly time series are indicated by fluctuating lines. Annual spring values are averaged from measurements in March to May (gray circles); annual fall values are averaged from measurements in September to November (gray squares). Multiyear trends in spring and fall are indicated by linear regression.

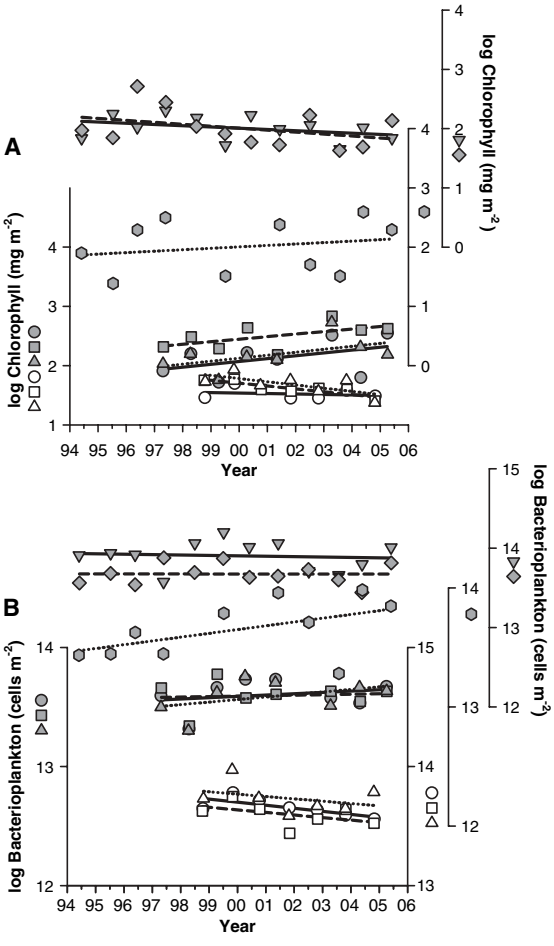

Fig. 2. Time series of log depth-integrated plankton variables showing station averages in various subregions. (**A**) Chlorophyll concentration. (**B**) Bacterioplankton abundance. Code for symbols: CSS spring, gray circle; ESS spring, gray square; WSS spring, gray triangle; CSS fall, white circle; ESS fall, white square; WSS fall, white triangle; LB spring, gray inverted triangle; LS spring, gray diamond; GS spring, gray hexagon. The appropriate ordinate for each time series in (A) and (B) is indicated by matching symbols on the *y* axes.

On the Scotian Shelf as a whole, depth-integrated chlorophyll has increased in the spring at about 12% per year and decreased in the fall at about –6% per year (Fig. 2A). With the exception of CSS in the fall, the changes in chlorophyll are significant ($P < 0.10$) at all other times and places (table S1). Analysis of covariance indicates the statistical equality ($P > 0.10$) of the rate of change for the stations within each subregion (table S1).

Independent support of these trends is provided by high-frequency satellite data. Season averages calculated from semimonthly composites of surface ocean color (Fig. 3, A to C) confirm the spring increases (average 9% per year) and fall decreases (average –2% per year) on the Scotian Shelf. Notwithstanding the weak statistical trends in individual time series, there is a strong correlation ($r = 0.82$, $P = 0.007$) between change indicated by in situ observations and remote observations (Fig. 4A). This correlation provides some confidence that the multiyear trends established by low-frequency sampling are not obscured by aliasing. Although it might appear remarkable that a semiannual sampling schedule could yield significant trends over a relatively small number of years, it should be noted that each in situ value for a particular subregion at any year (Fig. 2) embodies a great deal of environmental averaging by depth and stations. Depth-integrated station averages are tantamount to smoothing over vertical and horizontal space. Local contingencies are subsumed to better reveal any underlying trend. Strong local forces such as short-term wind-driven upwelling events (*9*) can overwhelm a small systematic trend, but spatial averaging generates more confidence in purported temporal change.

As a whole, these results point to a shelfwide trend of "spring-up and fall-down" in the intensity of chlorophyll. Historical measurements extend the springtime pattern backward. For example, depth-integrated chlorophyll on the Halifax Line in May 1974 averaged 33 ± 16 mg m^{-2} (*10*), a value considerably lower than the present-day spring average of 153 ± 115 mg m^{-2}. Additionally, data from institutional archives (*2*) indicate that at surface depths (<10 m), springtime chlorophyll on the shelf as a whole was significantly lower ($F_s = 7.99$, $P = 0.0075$; fig. S2A) from 1974 to 1981 (0.89 mg m^{-3}) than from 1996 to 2005 (2.0 mg m^{-3}). Finally, the green color index from the Continuous Plankton Recorder (*11*) also indicates significantly lower ($F_s = 14.1$, $P = 0.0005$; fig. S2B) springtime values from 1961 to 1976 (0.19 units) than from 1991 to 2003 (0.34 units). For reasons of methodology and the nature of phytoplankton, the color index cannot reliably predict chlorophyll concentrations (*12*, *13*). Furthermore, because the quantities are related to each other differently according to season (*13*), any comparison between spring and fall color indexes would not inform us of seasonal chlorophyll differences.

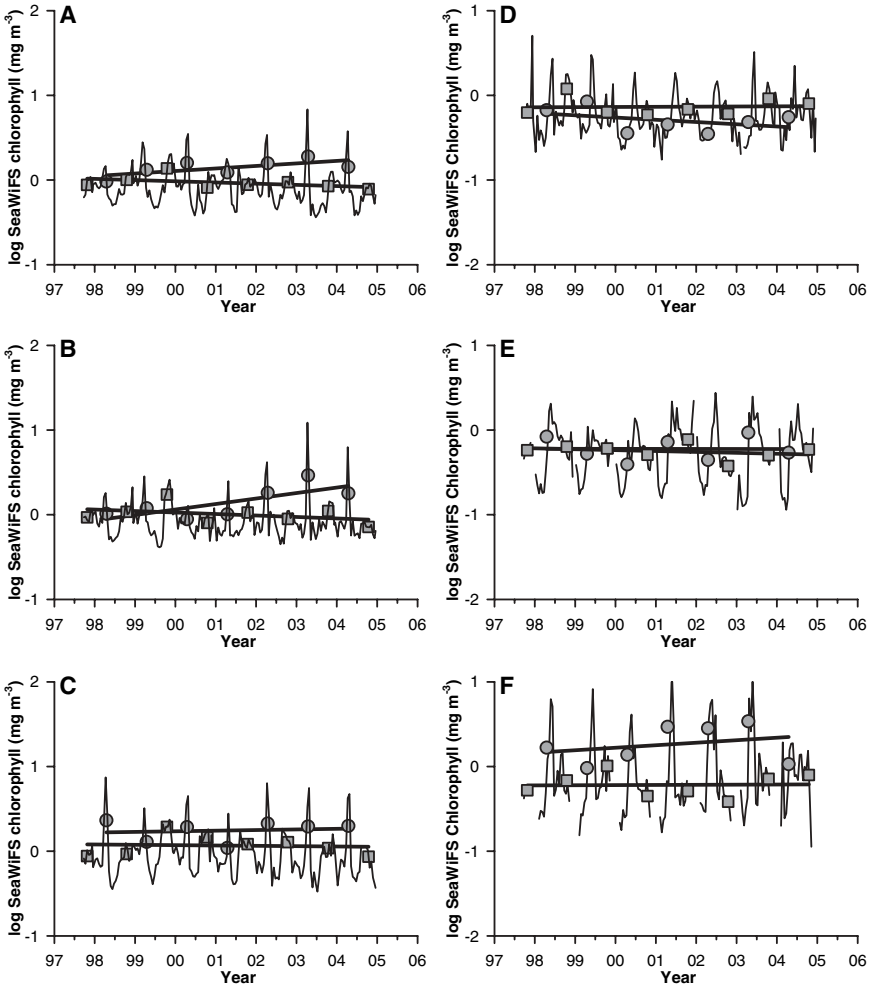

Fig. 3. Time series of log SeaWiFS satellite surface chlorophyll concentration in various subregions: (**A**) Central Scotian Shelf, (**B**) Western Scotian Shelf, (**C**) Eastern Scotian Shelf, (**D**) Labrador Shelf, (**E**) Labrador Basin, and (**F**) Greenland Shelf. Lines and symbols are as in Fig. 1B.

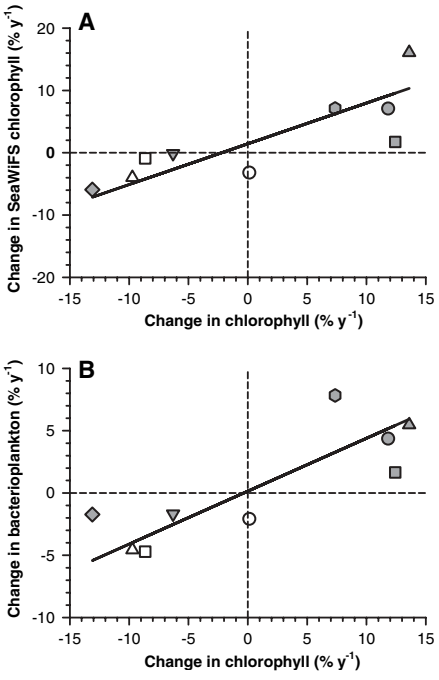

Fig. 4. Quadrant plots comparing multiyear change. (**A**) SeaWiFS satellite surface chlorophyll concentration versus in situ depth-integrated chlorophyll concentration. (**B**) Depth-integrated bacterioplankton abundance versus depth-integrated chlorophyll concentration. Code for symbols is as in Fig. 2.

On an annual basis, the opposing seasonal trends in chlorophyll on the Scotian Shelf largely cancel each other, yielding only small net changes (–1 to +3% per year) that are not statistically significant ($P > 0.50$). Elsewhere in other coastal oceans, a significant average increase (10% per year) of annual chlorophyll in recent years has been recorded and has been described as a possible response to enhanced coastal upwelling or anthropogenic influences (*14*). In the present regime on the Scotian Shelf, it can be said that apparent annual stability is the result of diverging but partially compensating changes in spring and fall. This small divergence could conceivably lead to an alternate regime if it were sustained for many years. Altered phytoplankton phenology has already been shown to affect higher trophic levels (*15*, *16*).

Turning now to the Labrador Sea subpolar gyre, we have a slightly longer record of observations here (1994 to 2005) for the spring, but none at all for the fall. Only on the GS has chlorophyll increased (Fig. 2A). Elsewhere in the gyre, there is a countertrend. Chlorophyll has undergone a significant springtime decrease of –13% per year on the LS and –6% per year in the LB (Fig. 2A). The direction of springtime change extracted from the high-frequency satellite record of ocean color matches in situ chlorophyll change in each subregion (Fig. 3, D to F, and Fig. 4A).

The opposite trends of chlorophyll in different seasons and subregions provide an opportunistic test of the hypothesized long-term linkage between phytoplankton and bacterioplankton. This is an experiment provided by nature. On the Scotian Shelf where there is "spring-up and fall-down" of chlorophyll, the same directional changes appear in bacterioplankton (Fig. 2B). The bacterial rates are modest: neither increasing more than 5% per year in spring, nor decreasing more than –5% per year in fall. In the Labrador Sea, the "spring-down" of chlorophyll is accompanied by a slight reduction of bacterioplankton (–2% per year) in both LS and LB. On the GS, chlorophyll and bacterioplankton have matched increases of about 7% per year (Fig. 2B).

In comparing bacterioplankton change (y) to chlorophyll change (x), the observations are found to lie exclusively in quadrant 1 ($x > 0$, $y > 0$) and quadrant 3 ($x < 0$, $y < 0$) (Fig. 4B). Thus, although bacterial change is statistically weak in individual subregions (table S1), it bears a strong correlation to chlorophyll change over a large area of the northwest Atlantic Ocean ($r = 0.83$, $n = 9$, $P = 0.006$). The reduced major axis slope of 0.42 ± 0.22 indicates that chlorophyll elicits a significantly dampened response from bacterioplankton. This is not surprising because chlorophyll has a much larger dynamic range than bacterioplankton in the ocean (*17*). It is known that marine bacterioplankton are highly diverse in phylogenetic affiliation, such that even the most common clade SAR11 (*Pelagibacter ubique*) comprises subclades or ecotypes that have different niches (*18*). Moreover, growth rates can differ greatly among phylogenetic groups such that group-specific increases can far exceed the bulk increase of the bacterial assemblage (*19*, *20*). The modest long-term bulk changes evidenced on the Scotian Shelf and Labrador Sea may be obscuring more significant change in the most active components of the microbial community.

The covariation between bacterioplankton and phytoplankton has been described as one of the few undisputed patterns in aquatic microbial ecology (*21*). The basis for this lies in the organic substrates supplied to the hetero-

trophs from the photoautotrophs. These substrates may be labile photosynthates exuded by phytoplankters, may be egesta released by grazers that have consumed phytoplankters, or may be cytoplasmic materials liberated by viral lysis or algal autolysis (*22*). The trophic groups are linked by a flux of organic matter; therefore, trophic covariation would most appropriately be sought from the carbon biomasses (mg C m^{-3}) of the two plankton groups. We have not measured carbon directly, choosing instead to represent the quantities by proxy: numerical abundance of bacterioplankton (*N*, cells m^{-3}) and chlorophyll concentration of phytoplankton (*Chl*, mg chlorophyll m^{-3}). A question inevitably arises: Are these proxies suitable to demonstrate trophic linkage, or are they inadequate because carbon biomass varies much more strongly with other factors such as cell size and pigment content, which change with physiological acclimation and taxonomic composition? On a seasonal basis, large differences may be evident in the carbon-to-chlorophyll ratio of phytoplankton, as well as in the carbon cell quota for bacterioplankton. Thus, multiyear analysis of *Chl* and *N* partitioned by seasons (Figs. 1 to 4) can be expected to be more robust because cellular parameters are more tightly constrained within seasons.

Notwithstanding seasonal differences in cellular parameters, extensive cross-ecosystem comparisons have repeatedly shown that $\log N \propto 0.46 \log Chl$ (*17*, *21*). This is a statistical trend describing the first-order relationship between the two proxies. There is much scatter of individual data about this trend, some of which can undoubtedly be explained by physiology and taxonomy. Nonetheless, the macroecological link between *N* and *Chl* through the exponent of 0.46 is consistent with the large-scale, multiyear damped response of *N* to *Chl* through the factor of 0.42 between their percentage changes (Fig. 4B).

Multiyear trends of *Chl* discerned from repeating annual cycles can be meaningfully interpreted in the context of climate variability (*14*, *23*). Trophic linkage of primary to secondary producers propagates the climate signal systemwide. Pelagic food webs in which phytoplankton are of small average cell size tend to be sustained by regenerated production, where a large fraction of energy loops through microbial components. Conversely, food webs in which phytoplankton are of large average cell size have a greater potential to transfer primary production to higher trophic levels (*24*). The ecosystem and biogeochemical implications of a long-term change in *Chl* depend on how phytoplankton biomass is packaged into discrete cells. Thus, an allometric approach (*25*) or a taxonomic approach (Fig. 1, C and D) to ecosystem monitoring yields important insights. For example, in the western subarctic North Pacific, a long-term decline in annual net community production is associated with a large springtime decrease in *Chl*, which in turn is due to a reduction in a particular subset of diatoms taxonomically identified as spring-type species (*1*).

A seasonal sign switch embedded in a multiyear phytoplankton trend has been documented elsewhere (*1*), but not, to our knowledge, a tandem sign switch in bacterioplankton. This is a compelling indication of trophic coupling at the temporal and spatial scales appropriate to climate change. The standing stock of chlorophyll is dependent on the stratification of the water column (fig. S3), implying that the observed changes are plausibly explained by changes in the delivery of deep nutrients to the surface. Within our data set, we are unable to discern a statistical correlation between the rate of change in chlorophyll versus the rates of change in temperature or the stratification index. However, much longer records of 30 to 40 years are often required to detect such linkages (*1*–*3*). Microbial observatories in the ocean directed toward long-term, spatially distributed investigations can be expected to contribute toward an understanding of ecosystem change.

References and Notes

1. S. Chiba, T. Ono, K. Tadokoro, T. Midorikawa, T. Saino, *J. Oceanogr.* **60**, 149 (2004).
2. K. T. Frank, B. Petrie, J. S. Choi, W. C. Leggett, *Science* **308**, 1621 (2005).
3. A. J. Richardson, D. S. Schoeman, *Science* **305**, 1609 (2004).
4. H. W. Ducklow, in *Ocean Biogeochemistry: The Role of the Ocean Carbon Cycle in Global Change*, M. J. R. Fasham, Ed. (Springer, New York, 2003), pp. 3–17.
5. C. Parmesan, G. Yohe, *Nature* **421**, 37 (2003).
6. J. C. Therriault *et al.*, *Can. Tech. Rep. Hydrogr. Ocean Sci.* **194**, 1 (1998).
7. J. Lazier, R. Hendry, A. Clarke, I. Yashayaev, P. Rhines, *Deep-sea Res. I* **49**, 1819 (2002).
8. See supporting material on *Science* Online.
9. B. J. W. Greenan, B. D. Petrie, W. G. Harrison, N. S. Oakey, *Cont. Shelf Res.* **24**, 603 (2004).
10. R. O. Fournier, J. Marra, R. Bohrer, M. Van Det, *J. Fish. Res. Board Can.* **34**, 1004 (1977).
11. D. Sameoto, *Can. J. Fish. Aquat. Sci.* **58**, 749 (2001).
12. G. C. Hays, J. A. Lindley, *J. Plankton Res.* **16**, 23 (1994).
13. S. D. Batte, A. W. Walne, M. Edwards, S. B. Groom, *J. Plankton Res.* **25**, 697 (2003).
14. W. W. Gregg, N. W. Casey, C. R. McClain, *Geophys. Res. Lett.* **32**, L03606 (2005).
15. T. Platt, C. Fuentes-Yaco, K. T. Frank, *Nature* **423**, 398 (2003).
16. M. Edwards, A. J. Richardson, *Nature* **430**, 881 (2004).
17. W. K. W. Li, E. J. H. Head, W. G. Harrison, *Deep-sea Res. I* **51**, 1529 (2004).
18. S. J. Giovannoni, U. Stingl, *Nature* **437**, 343 (2005).
19. Y. Yokokawa, T. Nagata, M. T. Cottrell, D. L. Kirchman, *Limnol. Oceanogr.* **49**, 1620 (2004).
20. R. R. Malmstrom, R. P. Kiene, M. T. Cottrell, D. L. Kirchman, *Appl. Environ. Microbiol.* **71**, 2979 (2005).
21. J. M. Gasol, C. M. Duarte, *FEMS Microbiol. Ecol.* **31**, 99 (2000).
22. T. Nagata, in *Microbial Ecology of the Oceans*, D. L. Kirchman, Ed. (Wiley-Liss, New York, 2000), pp. 121–152.
23. C. R. McClean, S. R. Signorini, J. R. Christian, *Deep-sea Res. II* **51**, 281 (2004).
24. J. J. Cullen, P. J. S. Franks, D. M. Karl, A. Longhurst, in *The Sea Vol. 12*, A. R. Robinson, J. J. McCarthy, B. J. Rothschild, Eds. (Wiley, New York, 2002), pp. 297–336.
25. W. K. W. Li, *Nature* **419**, 154 (2002).

26. We thank J. Anning, J. Bugden, C. Caverhill, P. Dickie, L. Harris, E. Horne, H. Maass, K. Pauley, T. Perry, C. Porter, and J. Spry for technical assistance, and A. Vezina for comments on the manuscript. Supported by the Program of Energy Research and Development, The Department of Fisheries and Oceans Strategic Science Fund in the Ocean Climate Program, and the Atlantic Zone Monitoring Program.

Supporting Online Material

www.sciencemag.org/cgi/content/full/311/5764/1157/DC1
Materials and Methods
Figs. S1 to S3
Table S1

17 November 2005; accepted 18 January 2006
10.1126/science.1122748

Dendritic Cell Apoptosis in the Maintenance of Immune Tolerance

Min Chen,[1*] Yui-Hsi Wang,[2] Yihong Wang,[2] Li Huang,[1] Hector Sandoval,[1] Yong-Jun Liu,[2] Jin Wang[1*]

Apoptosis in the immune system is critical for maintaining self-tolerance and preventing autoimmunity. Nevertheless, inhibiting apoptosis in lymphocytes is not alone sufficient to break self-tolerance, suggesting the involvement of other cell types. We investigated whether apoptosis in dendritic cells (DCs) helps regulate self-tolerance by generating transgenic mice expressing the baculoviral caspase inhibitor, p35, in DCs (DC-p35). DC-p35 mice displayed defective DC apoptosis, resulting in their accumulation and, in turn, chronic lymphocyte activation and systemic autoimmune manifestations. The observation that a defect in DC apoptosis can independently lead to autoimmunity is consistent with a central role for these cells in maintaining immune self-tolerance.

The critical role of apoptosis in maintaining peripheral tolerance is clearly demonstrated by systemic autoimmune diseases that result from mutations in the pro-apoptotic Fas receptor or Fas ligand genes, both in humans and mice (*1*–*3*). Although lymphocytes play a central role in these conditions, the extent to which apoptosis defects in various immune cell types might also be involved has yet to be fully characterized. Transgenic mice